DEUTSCHES ELEKTRONEN-SYNCHROTRON DESY

DESY 88-099
July 1988

MONTE CARLO STUDY OF STRUCTURE FUNCTION MEASUREMENTS AT HERA

by

G. Ingelman, R. Rückl

Deutsches Elektronen-Synchrotron DESY, Hamburg

ISSN 0418-9833

NOTKESTRASSE 85 · 2 HAMBURG 52

To be sure that your preprints are promptly included in the
HIGH ENERGY PHYSICS INDEX ,
send them to the following address (if possible by air mail) :

DESY
Bibliothek
Notkestrasse 85
2 Hamburg 52
Germany

DESY 88- 099
July 1988

ISSN 0418-9833

Monte Carlo Study of Structure Function Measurements at HERA[1]

G. Ingelman and R. Rückl
Deutsches Elektronen-Synchrotron DESY, Notkestrasse 85, D-2000 Hamburg 52, FRG

Abstract

Using Monte Carlo techniques we investigate possibilities to determine the shape in Bjorken-x of various structure functions and quark distributions from deep-inelastic $e^{\mp}p$ cross-sections measurable at HERA.

1 Introduction

Deep-inelastic lepton-nucleon scattering provides the most direct way to investigate the parton structure of the nucleon and, therefore, belongs to the main topics for experimental study at HERA. The prerequisite for a detailed determination of structure functions and quark distributions is a sufficiently precise and complete measurement of the differential cross-sections for the inclusive charged and neutral current scattering processes, $ep \to \nu_e X$ (CC) and $ep \to eX$ (NC). The results which can be expected from the H1 and ZEUS experiments are discussed for example in ref. [1]. At high energies or, more precisely, at very large momentum transfer the full structure of the electroweak interactions plays a role and, as a consequence, new structure functions enter the cross-sections. Also the quark representation of NC structure functions becomes somewhat more complicated than the familiar expressions valid at present-day energies. For this and other reasons, it is not totally straightforward to extract, from cross-section measurements at a fixed HERA energy, quark distributions for individual flavours or particular combinations of flavours, one might be interested in. Nevertheless, there are several possibilities. One can consider restricted kinematical regions where some of the structure functions are negligible or where the quark representation simplifies (e.g. valence quark approximation). More ambitiously, one can try to unfold particular quark distributions by combining data on different cross-sections. Clearly, each procedure has advantages and disadvantages. Some illustrative examples are described in refs. [2,3]. Which method is more suitable really depends on the data available and on the aim of the study, such as measuring the momentum distribution of a particular quark constituent or testing scaling violations predicted by QCD.

In the present paper, we investigate questions concerning the determination of the shape in Bjorken-x of various quark densities and structure functions in the kinematical range accessible to NC and CC measurements at HERA. In order to exploit the available statistics, the x-distributions can be averaged over y (or Q^2). As usual, the kinematical variables are defined by $Q^2 \equiv -q^2 = -(p_e - p_\ell)^2$, $y = P \cdot q / P \cdot p_e$ and $x = Q^2/2P \cdot q$, where p_e, p_ℓ, P denote the four-momenta of the incoming and scattered lepton and the incoming proton, respectively. The statistics of realistic event samples is simulated by Monte Carlo techniques, while detector effects are only taken into account by cuts in x, y and Q^2 within which the systematic shifts of the cross-sections are expected to be less than 10% [1].

[1] Contribution to the DESY workshop on Physics at HERA, Hamburg, October 1987.

The theoretical cross-sections used and the Monte Carlo procedures are specified in section 2. Taking an experimental approach we first, in section 3, illustrate approximate measurements of structure functions which can be obtained already with data on a single cross-section. In section 4, we then consider the more demanding extraction of particular quark distributions by combining different cross-sections. Because of the Q^2 evolution in QCD, x-distributions averaged over the y (or Q^2) range of HERA experiments are expected to differ in shape from the corresponding distributions at lower values of Q^2. We indicate the size of these effects and point out that, in some cases, a comparison of HERA results with low Q^2 data from present-day fixed target experiments should allow interesting QCD tests. Prospects of more stringent quantitative tests are discussed in ref. [3]. Finally, section 5 contains some remarks on the potential of HERA in exploring the region at $x \leq 0.01$, and some conclusions.

2 Theoretical Cross-sections and Monte Carlo Procedures

For our analysis we adopt the parton model expressions for the inclusive NC and CC cross-sections obtained in lowest order of the electroweak couplings and leading order QCD. Accordingly, the longitudinal structure funtion, being of next-to-leading order, is neglected. This approximation may affect our results for $x \lesssim 0.1$, but should not change our main conclusions. Furthermore, taking $Q^2 \gtrsim 100$ GeV^2 we can neglect target mass effects and higher twist contributions. Also, it is justified to assume four massless quark flavours (u, d, s, c). In fact, in a large part of the accessible (x, Q^2)-region at HERA, the contributions from charm and bottom quarks are expected to have a leading-log behaviour similar to that of light quarks, while top production is either negligible or directly observable [4]. Finally, for later applications it is convenient to factor out the dominant Q^2 dependences from the differential cross-sections.

In the NC case, we then define

$$\tilde{\sigma}_{NC}(e^{\mp}) \equiv \frac{Q^4}{4\pi\alpha^2}\frac{d\sigma_{NC}(e^{\mp})}{dx\,dQ^2} = \frac{1}{2x}\left[Y_+ F_2(x,Q^2) \pm Y_- xF_3(x,Q^2)\right] \tag{1}$$

where $Y_\pm \equiv 1 \pm (1-y)^2$ and α is the electromagnetic fine-structure constant. The NC structure functions

$$\begin{aligned} F_2(x,Q^2) &= \sum_f A_f(Q^2)\left[xq_f(x,Q^2) + x\bar{q}_f(x,Q^2)\right] \\ xF_3(x,Q^2) &= \sum_f B_f(Q^2)\left[xq_f(x,Q^2) - x\bar{q}_f(x,Q^2)\right] \end{aligned} \tag{2}$$

are linear combinations of quark and antiquark density distributions, $q_f(x,Q^2)$ and $\bar{q}_f(x,Q^2)$, having a logarithmic Q^2 dependence as predicted by QCD. The flavour-dependent coefficients

$$\begin{aligned} A_f(Q^2) &= e_f^2 - 2e_f v_e v_f P_Z + (v_e^2 + a_e^2)(v_f^2 + a_f^2)P_Z^2 \\ B_f(Q^2) &= -2e_f a_e a_f P_Z + 4v_e v_f a_e a_f P_Z^2 \end{aligned} \tag{3}$$

involve the electric charges e_f ($e_u = \frac{2}{3}, e_d = -\frac{1}{3}, etc.$), the NC vector and axial vector couplings, $v_f = [T_{3f} - 2e_f \sin^2\theta_W]/\sin 2\theta_W$ and $a_f = T_{3f}/\sin 2\theta_W$, and the ratio $P_Z = Q^2/[Q^2 + m_Z^2]$ of the Z and γ propagators. Quite obviously, T_{3f} denotes the third component of the weak isospin ($T_{3u} = \frac{1}{2}$, $T_{3d} = -\frac{1}{2}$, etc.) and θ_W is the Weinberg angle.

Similarly, we define rescaled CC cross-sections

$$\tilde{\sigma}_{CC}(e^{\mp}) \equiv \frac{4\sin^4\theta_W\,(Q^2 + m_W^2)^2}{\pi\alpha^2}\frac{d\sigma_{CC}(e^{\mp})}{dx\,dQ^2} \tag{4}$$

such that

$$\tilde{\sigma}_{CC}(e^-) = \sum_i \left[u_i(x,Q^2) + (1-y)^2 \bar{d}_i(x,Q^2)\right] \quad (5)$$
$$\tilde{\sigma}_{CC}(e^+) = \sum_i \left[\bar{u}_i(x,Q^2) + (1-y)^2 d_i(x,Q^2)\right]$$

where u_i and d_i denote the up- and down-type quark flavours (u,c) and (d,s), respectively. In the above and in what follows, we assume unpolarised $e^{\mp}p$ scattering.

One may have some objections against using lowest order expressions since it is known that (electromagnetic) radiative corrections to the differential cross-sections are quite important [5]. However, we do not see a reason why they cannot be properly calculated and subtracted off from the data. It is, therefore, understood to apply the above formulas to the data after these corrections.

In order to examine the prospects of extracting structure functions and particular quark densities from the measured differential cross-sections in a reasonably realistic way, we use Monte Carlo data samples that may simulate the real data obtainable in a few years of experimentation at HERA. By means of the Monte Carlo program LEPTO [6] sets of NC and CC events are generated corresponding to collisions of 30 GeV electrons and positrons with 820 GeV protons for an integrated luminosity of 200 pb^{-1} per lepton beam. This MC generator is based on the theoretical cross-sections given above with the parametrization 1 of Eichten et al. (EHLQ1) [7] for the input quark distributions and the values $\alpha = 1/137$, $\sin^2\theta_W = 0.226$ and $m_W = m_Z \cos\theta_W = 38.68\ GeV/\sin\theta_W$ for the electroweak parameters.

The number of events as well as the corresponding cross-sections are recorded in suitable bins of x and y. We note that for a given bin of y, the full range in x is kinematically allowed. Since we aim at the determination of x-distributions (and are not interested here in a detailed study of Q^2 dependences) it is thus advantageous to choose y, and not Q^2, as the second independent variable. In order to assure samples with reasonable statistics, the bin-size is increased as x and y increases. For y we have chosen six bins per decade which are equally large on a logarithmic scale, i.e. $\Delta \log y = 0.167$. In x we have taken bins with $\Delta x = 0.05$ for $x \leq 0.5$, $\Delta x = 0.1$ for $0.5 \leq x \leq 0.8$, and the bin $0.8 \leq x \leq 1$. For NC events we have in some cases exploited the high statistics available at low x and made a finer binning in the region $x \leq 0.1$. Although we mainly concentrate on the region $x \geq 0.01$, where data from fixed target experiments at comparatively low values of Q^2 already exist, we also exemplify the potential of HERA experiments in the very small x region, $10^{-4} \lesssim x \lesssim 10^{-2}$, where practically nothing is known so far.

Systematic errors arising from the energy calibration and resolution, granularity and beam hole of the detectors as well as other possible sources have not been included in our Monte Carlo simulation. However, these effects have been investigated in some detail by Feltesse in ref. [1]. There are, in principle, two ways to determine the values of x,y and Q^2 for a given event: either from an energy and angle measurement of the scattered electron or from the total hadron flow. The ranges of the above variables for which the systematic shifts of the differential cross-sections can be kept below 10% have been identified in ref. [1]. The 'safe' regions are

$$\textit{for electron measurements} \ : \ 5 \times 10^{-5} \leq x \leq 0.6\,, \ Q^2 \geq 5\ GeV^2\,, \ y \geq 0.1 \quad (6)$$
$$\textit{for hadron measurements} \ : \ 0.01 \leq x \leq 0.5\,, \ Q^2 \geq 100\ GeV^2\,, \ y \geq 0.03 \quad (7)$$

For NC events one can use both measurements, whereas CC events only allow measurements of the hadron flow. In order to make sure that our results based on statistical considerations are not spoiled by large systematic uncertainties, we impose cuts corresponding to eqs. (6) and (7) on the generated event samples. However, when we later plot distributions we also illustrate measurements at $x \geq 0.5$ or 0.6 which are expected to be affected by larger systematic errors.

3 Approximate Determination of Structure Functions

Already from data on a single differential cross-section one can determine certain structure functions to a good approximation. Suppose, in a first running period with an electron beam the NC and CC cross-sections $\tilde{\sigma}_{NC}(e^-)$ and $\tilde{\sigma}_{CC}(e^-)$ are measured. For sufficiently small values of Q^2, Z-exchange can be neglected relative to γ-exchange and, consequently, the NC structure function xF_3 vanishes, while F_2 reduces to the familiar electromagnetic structure function F_2^{em} as can be seen from eqs. (2) and (3). In this case, eq. (1) implies the approximate relation

$$\frac{2x}{Y_+}\tilde{\sigma}_{NC}(e^-) = F_2 + \frac{Y_-}{Y_+}xF_3 \;\approx\; F_2^{em} \equiv \sum_f e_f^2\,[xq_f + x\bar{q}_f] \tag{8}$$

In fact, the departure of F_2^{em} from the actually measured distribution on the left-hand side of the above relation is expected to be smaller than the statistical errors for a run of 200 pb^{-1}, as long as $Q^2 \lesssim 3000$ GeV^2 or $y \lesssim 0.3$.

Fig. 1 shows the shape in x of the quantity $\frac{2x}{Y_+}\tilde{\sigma}_{NC}(e^-)$ as obtained from the Monte Carlo event sample after performing a weighted average over the y-bins in the range $0.03 \le y \le 1$. Here, we have followed the usual procedure of averaging independent results $f(x,y_i)\pm\epsilon_i$ taking the errors as weights:

$$f(x) = \frac{\sum_i f(x,y_i)/\epsilon_i^2}{\sum_i 1/\epsilon_i^2} \;\;;\;\; \epsilon = \frac{1}{\sqrt{\sum_i 1/\epsilon_i^2}} \tag{9}$$

Also shown in Fig. 1 are theoretical distributions of $F_2^{em}(x,Q^2)$ for $Q^2 = 10, 10^2, 10^3$ and 10^4 GeV^2, evaluated directly from the quark densities [7] used in the Monte Carlo simulation. One can see that the NC cross-section, after simple renormalization, represents a rather good measurement of the electromagnetic structure function F_2^{em} at an average scale $Q^2 = 10^3$ GeV^2. We note that the high y bins, where the approximate relation (8) is not expected to be valid, have low statistics and thus contribute little to the average x-distribution calculated according to eq. (9). For instance, the result depicted in Fig. 1 does practically not change if y is restricted to $y \le 0.3$. Furthermore, measurements at $x \ge 0.6$ lost due to the cuts specified in eqs. (6) and (7) are indicated by open symbols. For the nominal integrated luminosity of 200 pb^{-1}, the statistical errors are smaller than the size of the symbols representing the MC data in Fig. 1, as can be seen from the last three points. Finally, we emphasize that by comparing the measurement anticipated for HERA with existing fixed target results one should be able to observe the QCD evolution in Q^2 even in the presence of some systematic uncertainties. This assertion is supported in Fig. 1 by showing the EMC data on F_2^{em} [8], which nicely follow the theoretical curve for $Q^2 = 10$ GeV^2. Thus, from a determination of the average x-distribution of F_2^{em} at HERA, using only NC e^-p data, one can expect interesting constraints on power-law scaling violations (from thresholds, formfactors, etc.) and an important test of QCD.

To proceed, the simultaneously measurable CC cross-section yields information on the following quark densities:

$$\tilde{\sigma}_{CC}(e^-) = u + c + (1-y)^2(\bar{d}+\bar{s}) \;\approx\; \begin{cases} u_v + \frac{1}{2}S & small\ y \\ u_v & large\ x \end{cases} \tag{10}$$

where eqs. (4) and (5) have been used, and u_v and S denote the valence up-quark and the total quark-antiquark sea, respectively. In Fig. 2, the Monte Carlo results on $x\tilde{\sigma}_{CC}(e^-)$, again averaged over y as described before, are plotted and compared to the theoretical momentum distributions for u_v and $u_v + \frac{1}{2}S = u + \bar{d} + \bar{s} + c$ at various values of Q^2. We see that, for $x \ge 0.15$, $x\tilde{\sigma}_{CC}(e^-)$ provides a good measurement for the x-distribution of $u_v + \frac{1}{2}S$ at an average scale $Q^2 \simeq 10^4$ GeV^2. At lower values of x, where the sea is dominant, $\tilde{\sigma}_{CC}(e^-)$ deviates from $u_v + \frac{1}{2}S$ due to the factor

$(1-y)^2$ in eq. (10) which leads to a suppression of the down and strange sea contribution at higher values of y. In fact, if one imposes a suitable cut on y, for example, $y \leq 0.1$, one can extend the measurement of $u_v + \frac{1}{2}S$ to the low-x region in Fig. 2a at the cost of larger statistical errors. On the other hand, at sufficiently large values of x only valence quarks are important and, thus, $\tilde{\sigma}_{CC}(e^-)$ can simply be identified with u_v. Unfortunately, the requirements for CC measurements specified in eq. (7) limit x from above. Nevertheless, as indicated in Fig. 2b, useful constraints on u_v at $Q^2 \simeq 10^4$ GeV^2 are obtained in the region $0.25 \leq x \leq 0.5$. Moreover, one can see that also in the CC case evolution effects may be observable when HERA results are compared with similar measurements from fixed target experiments. Although both the data expected from HERA and the existing fixed target results [9] have larger uncertainties than in the case of F_2^{em}, it should be possible to establish a significant difference in the valence quark region. This is exemplified in Fig. 2b for two representative measurements of xu_v [10,11] at low Q^2.

Quite obviously, runs with positrons would provide additional information. From $\tilde{\sigma}_{NC}(e^+)$ one can reproduce F_2^{em}, while $\tilde{\sigma}_{CC}(e^+)$ yields an approximate measurement of $d_v + \frac{1}{2}S$ and constraints on the valence down-quark distribution d_v [3,12]. However, once data from e^-p and e^+p collisions are available one can actually do much more. Some of the possibilities are described next.

4 Unfolding Structure Functions From Cross-Sections

After a few years of running and about equal time sharing between electron and positron beams one can try to unfold various quark distributions by combining data on $e^\mp p$ NC and CC cross-sections. On the one hand, this procedure circumvents approximations such as the ones considered in the last section, and thus permits a more detailed and complete determination of structure functions, at least in principle. On the other hand, it requires considerable higher statistics in order to yield accurate results. Moreover, one has to overcome usual problems with the relative normalization of data obtained under different experimental conditions. Below, we describe two examples for what one can expect from HERA (see also ref. [2,3,12]) assuming that the above problems can be solved and that the collected $e^\mp p$ luminosity amounts to 200 pb^{-1} for each lepton charge.

Using the theoretical expressions for the various cross-sections given in section 2 one readily derives the following relations for the valence up-quark density $u_v(x,Q^2)$ and the total singlet structure function $F_s(x,Q^2)$:

$$\begin{aligned} u_v(x,Q^2) &= f_1^{u_v}\left\{\tilde{\sigma}_{NC}(e^-) - \tilde{\sigma}_{NC}(e^+)\right\} + f_2^{u_v}\left\{\tilde{\sigma}_{CC}(e^-) - \tilde{\sigma}_{CC}(e^+)\right\} \qquad (11) \\ f_1^{u_v} &= \frac{(1-y)^2/Y_-}{(1-y)^2 B_u + B_d} \;;\; f_2^{u_v} = \frac{B_d}{(1-y)^2 B_u + B_d} \end{aligned}$$

and

$$\begin{aligned} F_s(x,Q^2) &\equiv \sum_f [xq_f + x\bar{q}_f] = x f_1^s\left\{\tilde{\sigma}_{NC}(e^-) + \tilde{\sigma}_{NC}(e^+)\right\} + x f_2^s\left\{\tilde{\sigma}_{CC}(e^-) + \tilde{\sigma}_{CC}(e^+)\right\} \qquad (12) \\ f_1^s &= \frac{-Y_-/Y_+}{(1-y)^2 A_u - A_d} \;;\; f_2^s = \frac{A_u - A_d}{(1-y)^2 A_u - A_d} \end{aligned}$$

The quantities A_f and B_f are the flavour-dependent coefficients of the NC structure functions given in eq. (3). Evidently, similar relations hold for other quark distributions [2]. Here, we want to concentrate on u_v and F_s because of the particular theoretical interest in these cases, and leave other distributions for a more comprehensive study [12].

The relations (11) and (12) illustrate the manipulations which must be applied to the measured cross-sections in order to unfold the weak propagator effects and the flavour dependent γ and Z

couplings, and to extract particular quark distributions. The achievable accuracy clearly depends on the properties of the coefficient functions f_i. It is thus useful to discuss them briefly. For the valence up-quark case, $f_1^{u_v}$ is generally much larger than $f_2^{u_v}$ and, hence, the NC data are quite important for the determination of $u_v(x,Q^2)$ despite the smallness of the difference $\tilde{\sigma}_{NC}(e^-) - \tilde{\sigma}_{NC}(e^+)$, which is only sizeable at large Q^2. As a consequence, one expects the extraction of u_v according to eq. (11) to improve with increasing Q^2 until the number of events, which of course decreases with Q^2, becomes too small. In the singlet case, the coefficients f_1^s and f_2^s are rather small in size and, moreover, multiply sums of NC and CC cross-sections. The extraction of F_s is therefore a priori only limited by the decreasing statistics at large values of Q^2. Yet, the denominator $(1-y)^2 A_u - A_d$ of $f_{1,2}^s$ vanishes at $\tilde{y} = 1 - \sqrt{A_d/A_u} \approx 1 - |e_d/e_u| = 1/2$ and, hence, the procedure is not well defined in y-bins close to $\tilde{y} = 1/2$. However, this subtlety does not cause too big a problem since it can be avoided by simply applying a cut $y < \tilde{y}$ without much loss of statistics. Only if one wants to obtain F_s as a function of both x *and* Q^2 one has to be more careful [2].

The valence up-quark and the singlet distributions extracted by this method from the Monte Carlo data samples are shown in Figs. 3 and 4. As before, the distributions are first obtained in bins of y, with errors calculated by propagating the statistical errors through the relations (11) and (12). The distributions are then averaged over suitable regions in y using eq. (9). More specifically, since the statistical precision in $u_v(x,Q^2)$ improves with increasing Q^2 (or y), as already pointed out, we have disregarded the low-y region and averaged over $0.15 \leq y \leq 1$. Hence, the procedure should reproduce $xu_v(x,Q^2)$ at a rather large mean Q^2 value. This is indeed the case as can be seen from a comparison of the Monte Carlo result and the theoretical momentum distributions for u_v in Fig. 3. On the other hand, in the case of the singlet structure function $F_s(x,Q^2)$, we have not used the high-y region because of the instability of the unfolding relation (12) at $y \approx 1/2$ and have thus averaged over $0.03 \leq y \leq 0.3$. Fig. 4 shows that the theoretically expected distribution for $F_s(x,Q^2)$ is well reproduced with $Q^2 \approx 10^3$ GeV^2.

As anticipated, combining data on different cross-sections, in order to extract particular quark momentum distributions, results in larger statistical (and systematic) errors than the approximate determination of certain structure functions from a single cross-section. This can be seen by comparing Figs. 3 and 4 with Figs. 1 and 2. Nevertheless, the achievable statistical accuracy is sufficient to observe the changes in shape predicted by QCD, when going from $Q^2 \approx 10$ GeV^2, typical for existing measurements, to $Q^2 \approx 10^3$ to 10^4 GeV^2, characteristic for the proposed HERA experiments. This expectation is corroborated in Fig. 3, where our results are confronted with fixed target data on xu_v. The crucial point is obviously the relative normalization of the two measurements. In the case of F_s, a similar comparison is more significant [12]. A great advantage of the unfolding procedure is its applicability in the whole accessible x-region. In particular, the determination of $xu_v(x)$ down to small x is really remarkable when compared to the rather restricted measurement illustrated in Fig. 2.

5 Summary

The study of deep-inelastic structure functions and quark distributions is one of the main experimental issues at HERA. Here, we have investigated possibilities to extract various interesting distributions from the NC and CC cross-sections and to determine their shape in x, averaged over y (or Q^2). It is important to note that the ep centre-of-mass energy is assumed to be fixed at the nominal value $\sqrt{s} = 314$ GeV. Furthermore, we have concentrated to the kinematical region at $x \geq 0.01$ and $Q^2 \geq 100$ GeV^2, which is accessible to NC and CC measurements and where it appears feasible to keep the systematic errors on the differential cross-sections below 10%. The achievable statistical accuracy is illustrated assuming an equal integrated luminosity of 200 pb^{-1} for e^-p and e^+p collisions. Our main results can be summarised as follows:

(i) A few quark distributions can be determined directly from single NC and CC cross-sections with a very good statistical precision. Particularly favourable cases are $F_2^{em} = \sum_f e_f^2[xq_f + x\bar{q}_f]$ and, for $x \gtrsim 0.15$, $xu_v + \frac{1}{2}xS$.
(ii) Other quark distributions can be extracted by combining e^-p and e^+p cross-sections. This procedure is, in principle, superior to the approximate methods *(i)*, but it is affected by larger experimental uncertainties. Nevertheless, one can unfold several distributions with quite a satisfactory or, at least, reasonable statistical accuracy, for example, xu_v and $F_s = \sum_f[xq_f + x\bar{q}_f]$.
(iii) The methods considered yield x-distributions at a mean Q^2 scale of 10^3 to 10^4 GeV^2. A comparison of such average x-distributions measurable at HERA with existing data from fixed-target experiments should allow to check the global pattern of the evolution in Q^2 expected in QCD. Particularly promising cases, in this respect, are F_2^{em} and F_s.

Of course, in order to study scaling violations in more detail and perform quantitative QCD tests one has to determine the x *and* Q^2 dependence of structure functions. This task is obvioulsy more difficult. Some possible approaches are discussed in ref. [3]. On the other hand, it should be comparatively easy to explore the physics at very small values of x, below $x \simeq 0.01$. In fact, by measuring the momentum of the scattered electron in NC events one expects to reach values of x as low as 10^{-4} [1]. In this region, $e^{\mp}p$ scattering is completely dominated by γ-exchange. Consequently, the cross-section is very large and should allow a rather detailed study of the relevant structure functions. Just to illustrate the statistical precision one can expect, we have extrapolated the cross-section $\tilde{\sigma}_{NC}(e^-)$ given in eqs. (1) to (3) to very small values of x keeping $Q^2 \geq 5$ GeV^2 as suggested by eq. (6). The result is shown in Fig. 5 for three representative Q^2 bins. The statistical errors, corresponding to an integrated luminosity of 10 pb^{-1}, are indicated by 'inverse' error bars in case they are smaller than the size of the symbols representing the Monte Carlo data in Fig. 5. Measurements satisfying also the remaining kinematical conditions of eq. (6), namely $y \geq 0.1$, are emphasized by full symbols. The sensitivity in this yet unexplored region is truly remarkable. This is also underlined by extrapolations of various conventional parametrizations for $F_2^{em}(x, Q^2)$, which more or less coincide for $x \geq 0.1$ but deviate from each other quite significantly at $x \leq 0.1$. Theoretical considerations suggest that at very samll x the structure functions may in fact behave drastically different from any of these extrapolations [13], and that the renormalization group improved quark parton model description may even break down altogether [14]. At any rate, one can expect very interesting results from HERA on these questions.

Acknowledgements. We thank J. Blümlein, F. Eisele, M. Glück and E. Reya for interesting discussions and helpful suggestions.

References

[1] J. Feltesse, these proceedings

[2] G. Ingelman, R. Rückl, Phys. Lett. 201B (1988) 369

[3] J. Blümlein, M. Klein, Th. Naumann, T. Riemann, these proceedings

[4] M. Glück, R.M. Godbole, E. Reya, Z. Phys. C38 (1988) 441
M. Glück, these proceedings

[5] Report of the study group on radiative corrections, these proceedings

[6] G. Ingelman, LEPTO version 5.2, DESY preprint in preparation

[7] E. Eichten, I. Hinchliffe, K. Lane, C. Quigg, Rev. Mod. Phys. 56 (1984) 579, ibid. 58 (1986) 1047

[8] J.J. Aubert et al., EMC Collaboration, Nucl. Phys. B259 (1985) 189

[9] For a recent compilation of data see, e.g.
T. Sloan, Proc. Int. Europhysics Conference on High Energy Physics, Uppsala, Sweden 1987, Ed. O. Botner, European Physical Society, Vol II, p. 857

[10] D. Allasia et al., WA25 Collaboration, Z. Phys. C28 (1985) 321

[11] H. Abramowicz et al., CDHS Collaboration, Z. Phys. C25 (1984) 29

[12] G. Ingelman, R. Rückl, DESY preprint in preparation

[13] M. Glück, R.M. Godbole, E. Reya, University of Dortmund preprint DO-TH 88/9

[14] L.V. Gribov, E.M. Levin, M.G. Ryskin, Phys. Rep. 100 (1983) 1

[15] D.W. Duke, J.F. Owens, Phys. Rev. D30 (1984) 49

[16] M. Glück, E. Hoffmann, E. Reya, Z. Phys. C13 (1982) 119

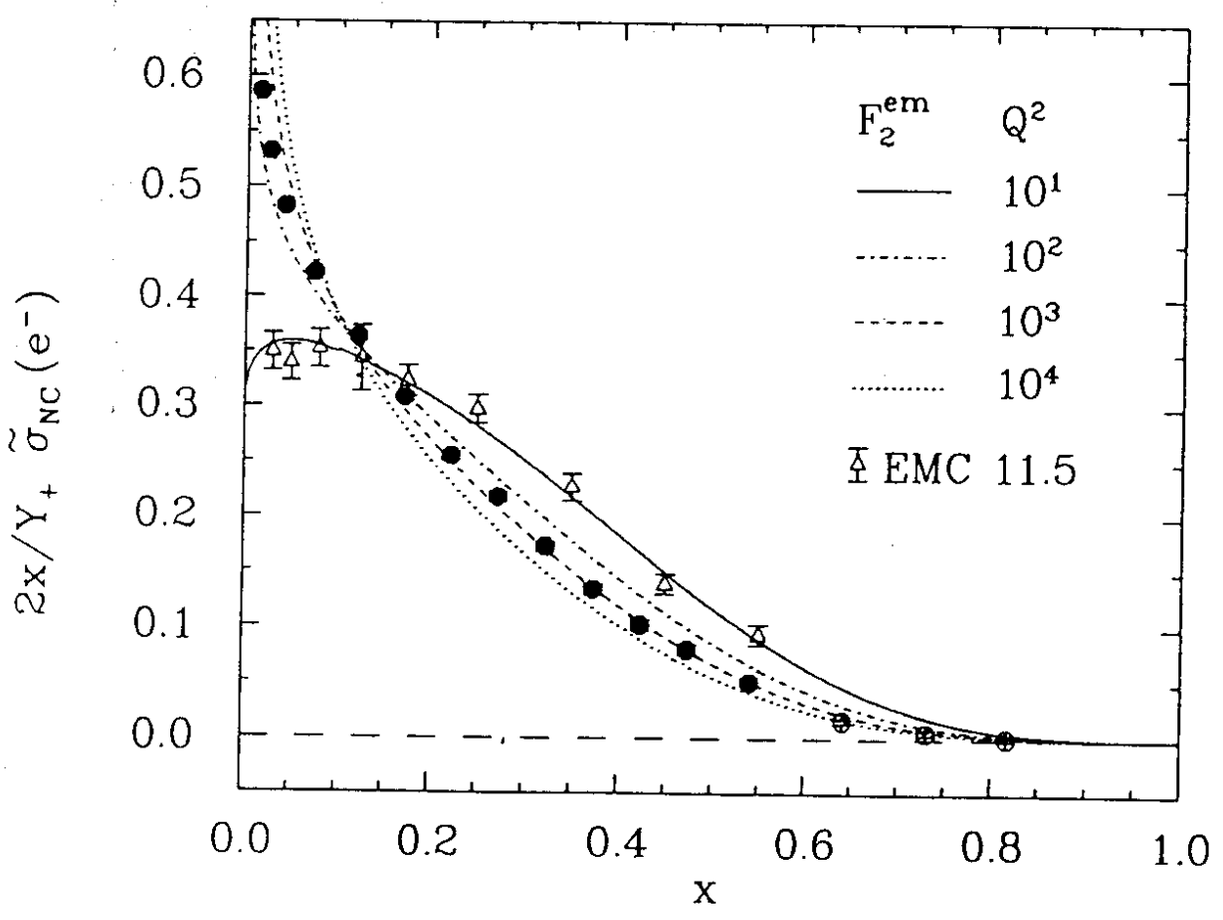

Figure 1 Approximate determination of $F_2^{em} = \sum_f e_f^2 [xq_f + x\bar{q}_f]$ from the NC cross-section for $e^- p$ scattering, averaged over $0.03 \leq y \leq 1$. The Monte Carlo data correspond to an integrated luminosity of 200 pb^{-1} and are drawn as full circles in case the phase space restrictions eqs. (6) or (7) are satisfied. The curves show $F_2^{em}(x, Q^2)$ for various values of Q^2 (in GeV^2), as evaluated from the input distributions [7]. The open triangles are EMC data on F_2^{em} [8] (statistical and systematic errors added in quadrature).

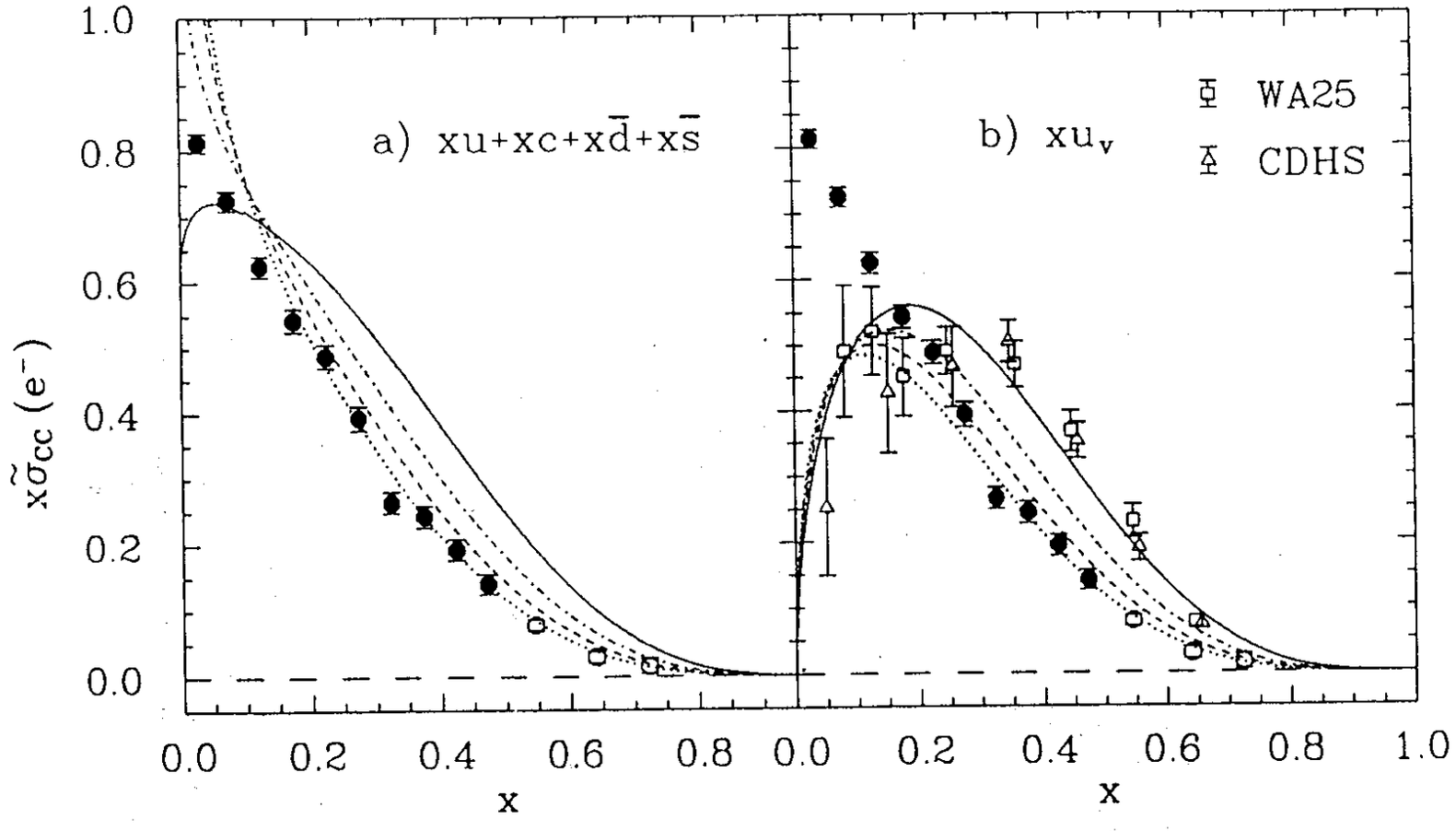

Figure 2 Approximate determination of $x(u + c + \bar{d} + \bar{s})$ and xu_v from the CC cross-section for $e^- p$ scattering, averaged over $0.03 \leq y \leq 1$. The Monte Carlo data correspond to an integrated luminosity of 200 pb^{-1} and are drawn as full circles in case the phase space restrictions eq. (7) are satisfied. The curves show (a) $x(u+c+\bar{d}+\bar{s})(x, Q^2)$ and (b) $xu_v(x, Q^2)$, as evaluated from the input distributions [7] for $Q^2 = 10$ (full), 10^2 (dash-dotted), 10^3 (dashed) and 10^4 (dotted) GeV^2. Also plotted in (b) are existing measurements of xu_v at $Q^2 = 11$ GeV^2 [10] (open squares) and $Q^2 = 15$ GeV^2 [11] (open triangles).

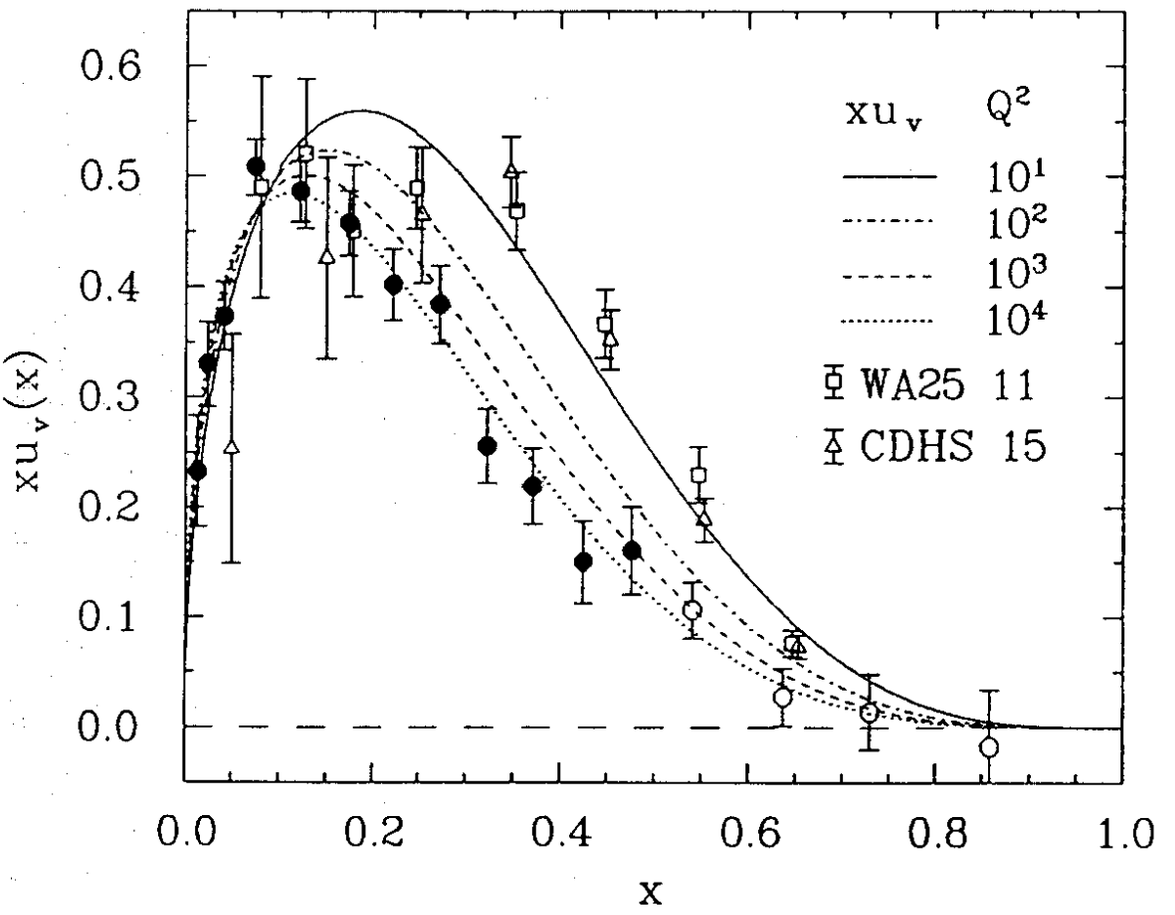

Figure 3 Extraction of the valence up-quark distribution xu_v from the NC and CC cross-sections for e^-p and e^+p scattering. The Monte Carlo results are averages over $0.15 \leq y \leq 1$ and correspond to an integrated luminosity of 400 pb^{-1} shared equally between e^- and e^+ runs. The Monte Carlo data are drawn as full circles in case the phase space restrictions eq. (7) are satisfied. The curves show $xu_v(x, Q^2)$ for various values of Q^2 (in GeV^2), as evaluated from the input distributions [7]. Open squares and triangles are fixed target data on xu_v at low Q^2 [10,11].

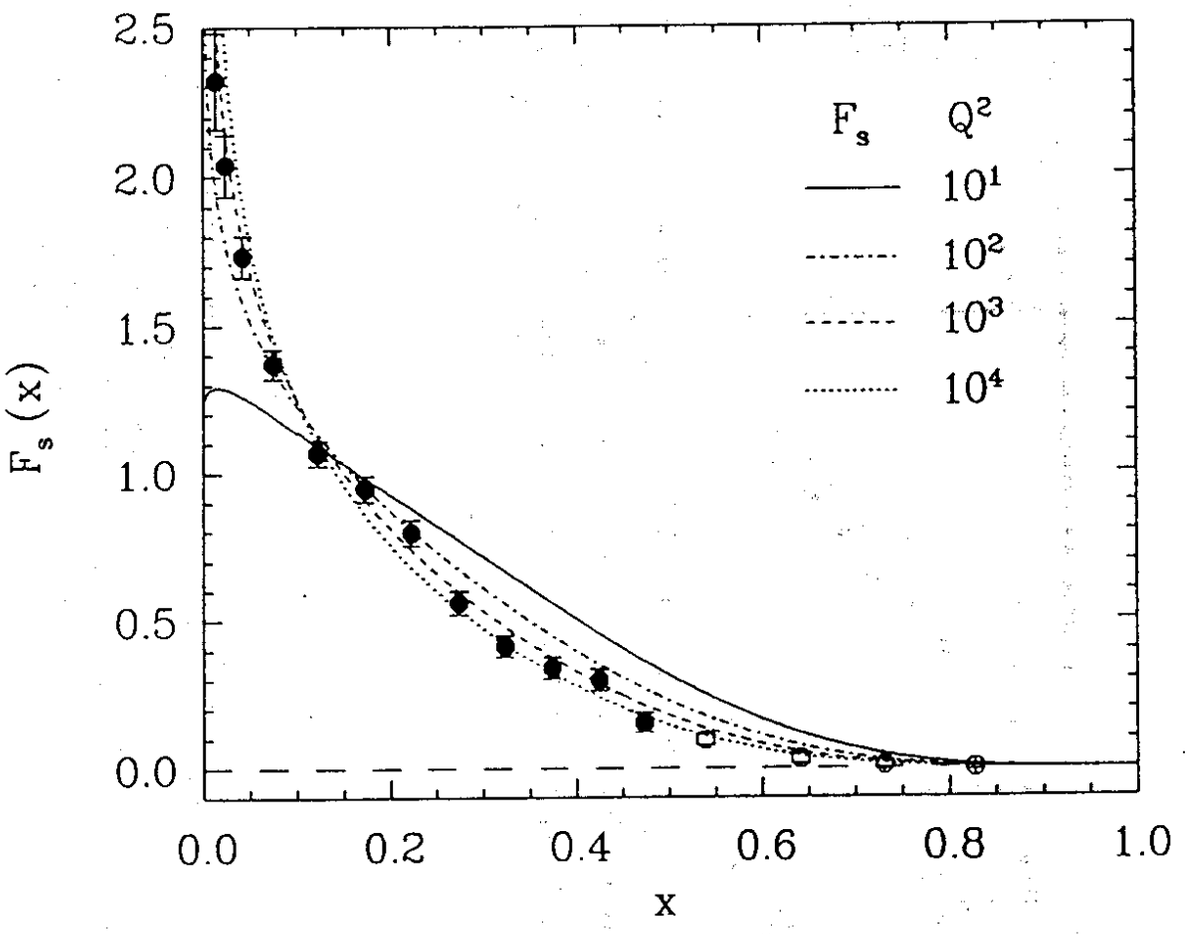

Figure 4 Extraction of the singlet structure function $F_s = \sum_f [xq_f + x\bar{q}_f]$ from the NC and CC cross-sections for $e^- p$ and $e^+ p$ scattering. The Monte Carlo results are averages over $0.03 \leq y \leq 0.3$ and correspond to an integrated luminosity of 400 pb^{-1} shared equally between e^- and e^+ runs. The Monte Carlo data are drawn as full circles in case the phase space restrictions eq. (7) are satisfied. The curves show $F_s(x, Q^2)$ for various values of Q^2 (in GeV^2), as evaluated from the input distributions [7].

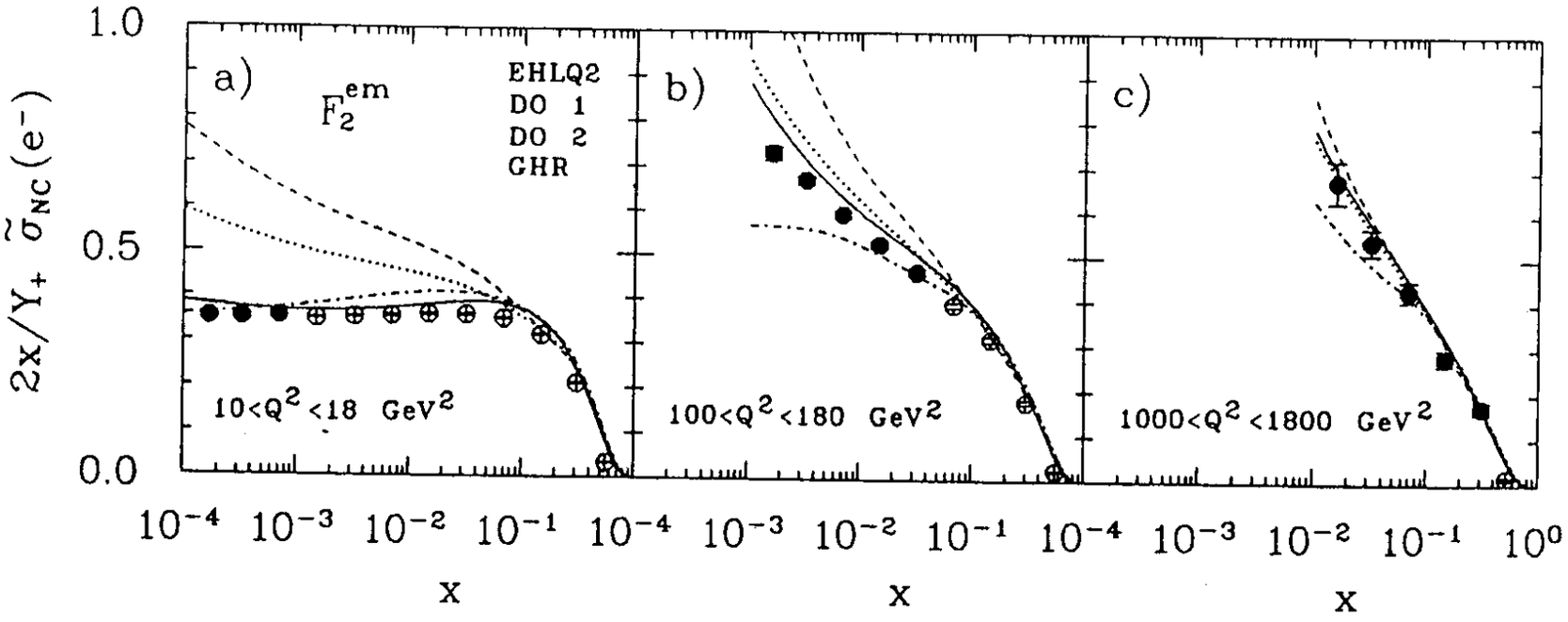

Figure 5 Extrapolation of the differential NC cross-section to very small values of x, in terms of conventional structure functions as given by the EHLQ1 parametrization [7]. The Monte Carlo data correspond to an integrated luminosity of 10 pb^{-1} and are drawn as full circles in case the phase space restrictions eq. (6) are satisfied. Also shown are the theoretical expectations for $F_2^{em} = \sum_f e_f^2[xq_f + x\bar{q}_f]$ based on other parametrizations of quark distributions: EHLQ 2 (full) [7], DO 1 (dotted) and DO 2 (dashed) [15], GHR (dash-dotted) [16].